RSC Advances




ROYAL SOCIETY OF CHEMISTRY

www.rsc.org/advances

# Transfer of vertically aligned carbon nanotube arrays onto flexible substrates for gecko-inspired dry adhesive application

Yang Li,[a,b] Hao Zhang,[b] Yagang Yao,[*c] Taotao Li,[c] Yongyi Zhang,[c] Qingwen Li,[c] and Zhendong Dai,[*b]

[a] *College of Material Science and Technology, Nanjing University of Aeronautics and Astronautics, Nanjing 210016, China.*

[b] *Institute of Bio-inspired Structure and Surface Engineering, College of Astronautics, Nanjing University of Aeronautics and Astronautics, Nanjing 210016, China.*

[c] *Key Laboratory of Nanodevices and Applications, Suzhou Institute of Nano-tech and Nano-bionics, Chinese Academy of Sciences, University of Chinese Academy of Sciences, Suzhou 215123, China.*



[*c] Corresponding author. Tel: +86-512-62872829; Fax: +86-512-62872552;E-mail: ygyao2013@sinano.ac.cn (Y. Yao).
[*b] Corresponding author. Tel: +86-025-84892584; Fax: +86-025-84892581;E-mail: zddai@nuaa.edu.cn (Z. Dai).

**Abstract:** Gecko's extraordinary climbing ability has inspired scientists to develop synthetic dry adhesives by mimicking the structure and function of gecko feet. Vertically aligned carbon nanotube (VACNT) array has been considered as a potential candidate for developing gecko-inspired dry adhesive materials due to the outstanding structural and mechanical properties. However, the limited choices of growth substrates and poor interfacial bonding between VACNTs and growth substrates have restricted their application as gecko-inspired dry adhesive materials. Here, we report a versatile transfer method for transferring VACNT arrays onto flexible polymer substrates by using a thermal oxidation process. This transfer method mainly focused on using the VACNT array as a gecko-inspired dry adhesive. With the transferred method developed in our study, VACNT array-based gecko-inspired dry adhesive materials with improved adhesion property, structural stability, and self-cleaning ability can be developed. A thermal oxidation process was used to obtain freestanding VACNT arrays, resulting in the production of top-transferred and bottom-transferred structural VACNT array-based dry adhesive materials. Shear adhesive strength of the transferred VACNT array was enhanced with this method. The interfacial bonding strength of the transferred VACNT array increased nearly 15 times with nanoscratch tests. The flexible structure of the transferred VACNT array showed a better nonfouling state by mimicking the digital hyperextension (DH) motion, which is a natural peeling motion of the gecko foot with a unique dynamic self-cleaning mechanism. These findings show that our method is an efficient method for transferring VACNT arrays, an important process for fabricating gecko-inspired

VACNT array-based dry adhesive materials with great structural stability, self-cleaning ability , and high adhesive strength.

## 1. Introduction

Gecko has excellent climbing ability and can move freely on almost any surface-flat or inclined. The chief reason for gecko's extraordinary climbing ability is that its toes are covered with a hierarchical structure of compliant β-keratin hairs comprising mesoscale lamellae, microscale seta, and nanoscale spatula; these hairs can integrate weak van der Waals (vdW) force into a sufficiently strong adhesive force.[1-3] Gecko's locomotion and hierarchical structural adhesive systems have been extensively researched and the results have been used in fabricating gecko-mimetic climbing robots, which can perform many useful tasks such as surveillance, inspection, repair, and cleaning; they can even work in the space environment.[4-6] In order to mimic gecko's super-climbing ability in robots, it is imperative to develop a new class of gecko-inspired dry adhesive materials that are not only sticky but also structurally stable, adaptable, and reusable.[7] In recent years, synthetic polymers,[8,9] and vertically aligned carbon nanotube (VACNT) arrays,[10-12] have been developed as two major types of materials for producing gecko-inspired dry adhesive materials. Initially, polymers were used as gecko-inspired dry adhesive materials because of their structural versatility (such as polyurethane micropillars with angled mushroom tips, and micro/nanoscale hierarchical polymeric hairs[13,14]) and simple fabrication processes (cast-molding or lithography[15,16]). However, they have many limitations such as poor mechanical and structural properties. In contrast, VACNT arrays are not

only structurally similar to gecko foot hairs, but are also endowed with additional outstanding mechanical,[17] chemical,[18] electrical,[19,20] and thermal properties,[21] and hence, they are considered as a potential candidate for advanced gecko-inspired dry adhesive materials. An adhesive strength of more than 500 N/cm$^2$ between the VACNT array and a glass surface has been theoretically predicted.[22,23] Qu et al.[10] have fabricated hierarchically structural VACNT array with a curly entangled top layer and generated a macroscopic adhesive strength of around 100 N/cm$^2$, nearly 10 times more than that of natural seta array on one toe of a gecko foot, which is so far the highest adhesive strength reported for VACNT array-based dry adhesive materials. Chemical vapor deposition (CVD) is commonly used to synthesize VACNT arrays. Considering the high growth temperature (around 750 °C) involved and the requirement of a buffer layer ($Al_2O_3$) on the top of the growth substrate during the CVD reaction process, high-melting-point semiconductors (e.g. Si) and insulators (e.g. quartz) are considered as optimal substrates for VACNT growth.[24] However, poor interfacial bonding between the VACNT array and silicon substrates may cause unreliable behavior and reduced structural stability, reducing the life span of VACNT arrays as dry adhesives.[25] In addition, compared with the robust and flexible gecko toe pads on which all the hierarchical hairs are oriented and distributed in a similar fashion,[26] the silicon substrate is stiff, brittle, and fragile, thus decreasing the adaptability of VACNT array-based dry adhesive materials. Therefore, it is highly desirable to develop a versatile method for transferring VACNT arrays from the growth substrates onto flexible substrates for achieving gecko-inspired dry adhesive

applications.

Recently, a few methods have been developed to transfer VACNTs onto different substrates. Ahmed et al.[27] reported the fabrication of high-quality and stable carbon nanotube (CNT) films on flexible substrates through the spray deposition method, but the CNTs so obtained exhibit randomly oriented morphology. Jani et al.[28] adopted a solder transfer method for finned CNT structures. Thin films of Cr/Au were deposited on CNT tips to enhance the successful transfer of CNT films to the Ag solder pads of ceramic chips, which is a complex and expensive process. Kang et al.[29] used a polydimethylsiloxane polymer as an intermedium to transfer the VACNT array, but the process has low efficiency and needs to be improved. Moreover, previous studies, especially those on polymer-based transfer technique of VACNT arrays, mainly focused on the electrical or field emission performance;[24,30] the mechanical performance was seldom investigated for the transferred VACNT arrays.

Geckos possess outstanding adhesive ability and also show nonfouling performance, which help them engage in durable walking under various environments. Hu et al.[32] studied the self-cleaning ability of geckos during locomotion and proposed an intrinsic dynamic self-cleaning mechanism associated with both the structure of gecko toe pad and their natural peeling motion called digital hyperextension (DH). During the hyperextended peeling, the setae on gecko foot roll up and detach from the substrate and then generate high inertial forces to separate dirt particles from the spatula. The recovery rate of adhesion ability of geckos with DH motion is two times higher than those without DH. Self-cleaning performance of the gecko-inspired dry

adhesive is a basic requirement for achieving a reusable and reliable application of gecko-mimetic robots. VACNT arrays as a potential dry adhesive candidate show structural similarity with the gecko foot hairs.[10] However, VACNT arrays grown on a rigid silicon substrate are not suitable to realize the peeling and scrolling of the DH motion and thus could not realize the dynamic self-cleaning mechanism.

In this work, a fast, low cost, versatile, and easy to scale-up transfer method of VACNT arrays was developed to fabricate a gecko-inspired dry adhesive. An as-grown VACNT array was transferred onto a flexible polyethylene terephthalate (PET) substrate with thermoplastics polyurethane (TPU) intermediation after carrying out a brief thermal oxidation pretreatment of the VACNT arrays. Morphological and structural characterizations of the VACNT arrays were carried out both before and after the transfer.

## 2. Experimental section

### 2.1 VACNT array synthesis

The process of VACNT array growth mainly includes catalyst deposition and CNT precipitation. A $Si/SiO_2$ wafer was chosen as the growth substrate. A 20-nm-thick $Al_2O_3$ layer and a 2-nm-thick Fe film were deposited on the $Si/SiO_2$ substrate as catalysts by using an electron beam system (E-beam 500, Xingnan, Chengdu, China). Thermal CVD was used for growing VACNT arrays in a tubular furnace (OTF-1200X-80, Kejing, Hefei, China). For the entire reaction process, 1500 standard cubic centimeters per minute (sccm) Ar was used as the carrier gas. At nearly 650 °C, 500 sccm $H_2$ was injected into the furnace for catalyst pretreatment,

and a VACNT array was precipitated when 250 sccm $C_2H_2$ was introduced into the reactor at 720 °C. The reaction time was 3-30 min and the length of the VACNT array varied between 100 and 800 μm. When the growth ended, $C_2H_2$ and $H_2$ supply were stopped but Ar was kept flowing until the temperature decreased to room temperature.

**2.2 Transfer process of VACNT array**

TPU (Desmopan 786L, Bayer, Germany) was chosen as the transfer medium because of its high mechanical strength and good flexibility. The transfer process is illustrated schematically in Fig. 1a. TPU particles were dissolved in *N*,*N*-dimethyl formamide (DMF) solution (mass ratio 1:4) at 70 °C. The volume of the TPU solution was 100 μL. Then, a drop of the dissolved TPU solution (100 μL) was spin coated (KW-4A, IMECAS, China) on top of a flexible PET plastic sheet for use as the transferred substrate. The spin speed was set at 5000 rpm for 30 s. Meanwhile, the as-grown VACNT array was placed in the tubular furnace for a 5 min thermal oxidation pretreatment step (500 °C) in air, which assists in the detachment of the nanotube films from the Si substrates. After the detachment, the pretreated VACNT array can be transferred with either its top side (top transfer) or bottom side (bottom transfer) bonded to a PET plastic sheet under a normal pressure of ~0.5 N/cm$^2$. Then, this integrated structure was put into an oven at 70 °C for 15-30 min to polymerize TPU; finally, the flexible PET plastic sheet with the transferred VACNT array was peeled off.

**2.3 Characterization**

High-resolution field emission scanning electron microscopy (HR-FESEM,

HitachiS-4800, Japan) was used to characterize the morphology of the as-grown VACNT arrays at an operation voltage of 10 kV. Micro Raman spectroscopy (Raman, Labram HR 800, Japan) was used to characterize the quality (graphitic ordering, defects, etc.) of the VACNT arrays. The height of VACNT array was measured through Optical Microscopy (SK-2000H).

**2.4 Mechanical measurement**

To evaluate the adhesive properties of the VACNT arrays, two different evaluation systems were used. One is the hanging weight system, which is simple and intuitive. This system can directly suspend different weights to test the shear adhesive strength of VACNT arrays. VACNT array samples were attached to a plastic sheet by the 3M scotch tape and then finger-pressed onto a glass surface under a preload of nearly 40 $N/cm^2$. The end of the plastic sheet was hanged with different weights. The weights were increased until the detachment occurred.

The other one is the multifunctional material adhesion and friction test platform (IBSS-2, NBIT, Nanjing, China), which was used to accurately analyze the adhesive behavior of VACNT array-based dry adhesive materials. The platform contains a 2-dimensional force sensor with a force resolution of approximately 1 mN. An automated stage driven by the motor can be moved in both the vertical and horizontal directions to test the shear adhesive strength of VACNT array-based dry adhesive materials. A glass slide was used as an adhesive test surface and was mounted on a circular stage. A VACNT array was attached to the sample stage and it moved along with the force sensor. Firstly, when the top surface of the VACNT array was normally

encountered with the glass slide, a micro shear dragging process was implemented to help align the nonaligned and entangled CNTs along the shear direction, which could further increase the side-wall contact area.[10] Then, the VACNT array along with the sample stage was moved vertically with a constant speed of 5 μm/s, and then was compressed against the glass slide until the preload of ~18 N/cm$^2$ was achieved, after which the samples were released to achieve the normal preload of 0 N on the CNT sample. Without normally detached from the glass surface, the CNT samples were moved along the shear direction under no external compression until the stick-slip motion was observed during a dynamic friction process,[40] the force responses alone with the time were continuously recorded, which intuitively reflected the adhesive behavior of VACNT array-based dry adhesive material so that they can be used in practical applications such as the fabrication of a gecko-inspired climbing robot.[31]

The bonding strength between VACNTs and substrates were characterized through a nanoscratch-based technique proposed by Indranil et al.[25] The Nano Indenter (G200, Agilent, America) was used to quantify the bonding strength between VACNTs and two different substrates, Si and PET, one having $Al_2O_3$ and Fe as the buffer and catalyst layers, respectively, and the other having TPU as a transfer medium layer on top. VACNT array samples of height 100 μm were tested. A bare silicon substrate with $Al_2O_3$/Fe layers and PET substrate with a TPU layer were used as control groups. During scratching, a standard conical diamond tip (with 5-μm tip radius and 90° angle) was used with a normal preload of 150 μN. The length of each scratch was kept constant at 100 μm. The tip scratched from a bare surface and then

encountered the VACNT array. While moving through the VACNT array, the indenter tip faced an extra opposing force and uprooted the CNTs. Yu et al. have described the scratch process in detail.[23]

The nonfouling state of the VACNT array was realized through mimicking the DH pealing and scrolling motion of a gecko walking in a dirty environment.[32] Setae hairs of gecko foot could be scrolled up and spread out progressively from the substrate during the DH motion and if restricting their DH motion, gecko could lift their limbs to detach toes from the substrate, which was considered as limb motion (LM) by Hu et. al.[32] Silica particles, with diameters ranging from 5 to 10 μm, were used as the fouling agent in this study. The VACNT array samples (10 mm × 20 mm) were first covered with silicon particles (5-10 μm diameter) and then finger-pressed with a preload near 40 N/cm$^2$. A pair of tweezers was used to scroll and peel the transferred VACNT array samples to mimic the DH motion. Due to the limitation of the rigid silicon substrate, as-grown samples were directly detached from the substrate with tweezers in a crack-growth mode just like the LM motion of gecko.[32] Both of the motions were repeated for 10 times. The fouling state of VACNT arrays were examined and recorded by SEM.

## 3. Results and discussion

### 3.1 Transfer process of VACNT array

The structural integrity and stability of VACNT arrays are very important for their application as dry adhesive materials. However, when the transfer process is

carried out without any oxidation pretreatment, CNTs usually do not detach completely, always leaving some residues on the silicon substrate (Fig. S1 in the Supporting Information). Therefore, in our experiment, an additional oxidation pretreatment was introduced to help the complete transfer of the VACNT array. Fig. 1a schematically illustrates the transfer process of a VACNT array. Firstly, the synthesized VACNT array (Fig. 1b) was directly placed under a thermal oxidation environment in air at 500 °C for 10 min and then cooled down to room temperature. Thus, a freestanding VACNT array was removed with tweezers (Fig. 1c). The base-growth mechanism that the CNT continues to grow from the particles anchored to the substrate,[33] illustrates that the roots of the CVD-synthesized VACNT array get wrapped by the catalyst particles with a strong adherence to the surface of substrate. When the temperature was ~500 °C, the oxygen atoms would etch the carbon atoms near the root ends,[34-36] making the as-grown VACNT array (AC) much easier to detach from the silicon substrate. Secondly, a drop of TPU solution was spin coated (5000 rpm for 30 s) on the flexible plastic PET substrate. Thirdly, both the top and bottom sides of the freestanding VACNT array can be used as the new bonding interface. The top-transferred VACNT array (TC) and the bottom transferred VACNT array (BC) were integrated together under a normal pressure of about 0.5 N/cm$^2$. Finally, the TC and BC samples were obtained after the polymerization of TPU. The VACNT array transferred onto the flexible PET plastic sheet can be folded many times without any obvious structural damage, as shown in Figs. 1d and 1e. The flexible and foldable dry adhesive can help increase the real contact area on coming in

contact with uneven surfaces, as in the natural environment of geckos. Therefore, the transferred VACNT array can be beneficial in improving the flexibility and adaptability of VACNT array-based dry adhesive materials.

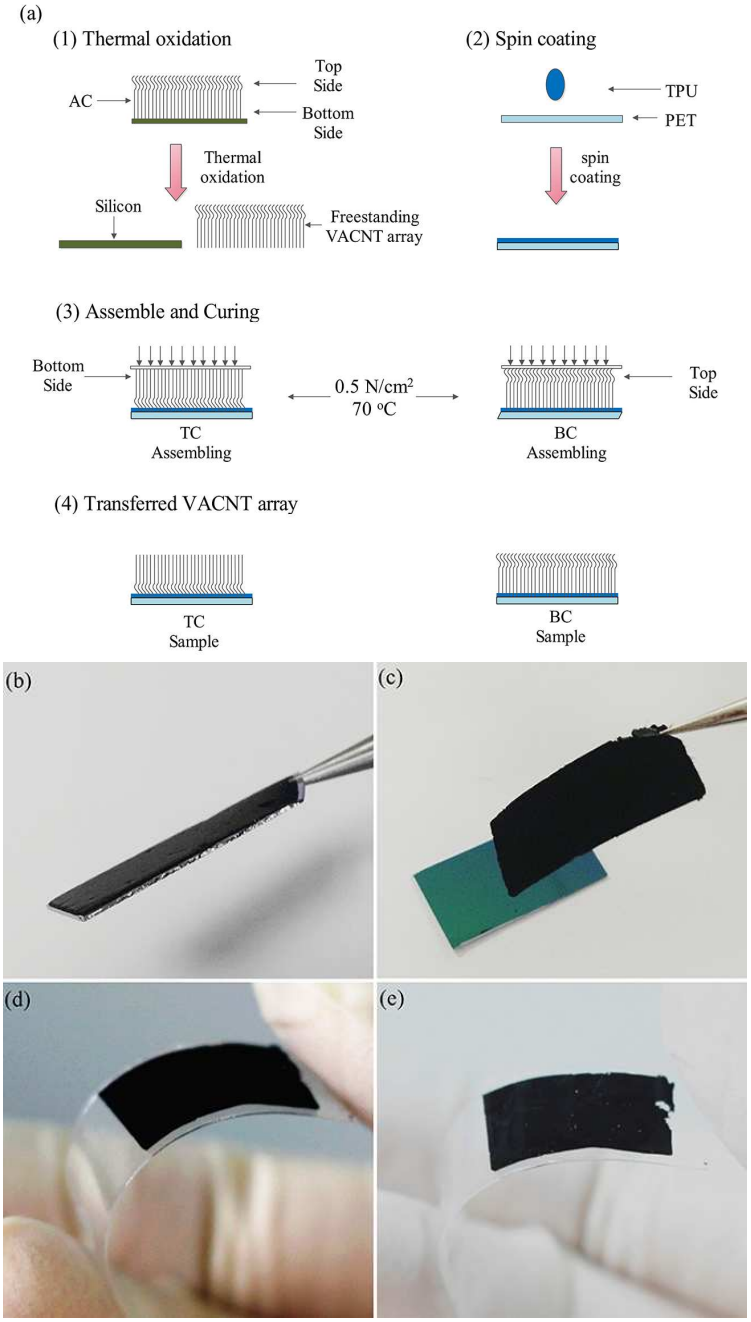


**Fig. 1** (a) Schematic of the transfer process of vertically aligned carbon nanotube (VACNT) array onto PET substrate: (1) thermal oxidation process of as-grown VACNT array (AC) at 500 °C for 10 min. (2) TPU layer was spin coated on PET

substrate. (3) Assemble of top-transferred VACNT array (TC) and bottom transferred VACNT array (BC) samples and curing in the oven at 70 °C for 15-30 min. (4) Transferred VACNT arrays; (b) Optical image of AC on silicon substrate; (c) Detached freestanding VACNT array after thermal oxidation process; Bending and scrolling of (d) TC sample and (e) BC sample.

In addition, the transfer method developed herein can be widely used to transfer VACNT arrays of different sizes onto various substrates such as copper foils, glass, and even paper, as shown in Fig. S2 in the Supporting Information. The concentration of the transfer medium shows obvious effects on the transfer results and thus needs to be optimized to obtain the structural integrity of the transferred VACNT array, as shown in Fig. S3 in the Supporting Information. The mass concentration of the TPU solution was set as 10%, 15%, 20%, and 25%. From the optical images shown in Fig. S3, it is clear that if the concentration of the TPU solution is low (10% and 15%), all CNTs cannot attach to the polymer layer and hence easily drop from the interface. At higher concentrations (25%), the entire VACNT array would be embedded in the polymer layer while some parts of the polymer would shrink, thus destroying the morphology of the top surface and the vertically aligned structure of the transferred array. Typically, the most appropriate concentration used was approximately 20 mass% TPU; with this concentration, the VACNT array can be firmly transferred onto the polymer interface and the vertically aligned structure is also maintained. Thus, 20 mass% TPU can be used to manufacture gecko-inspired dry adhesive materials.

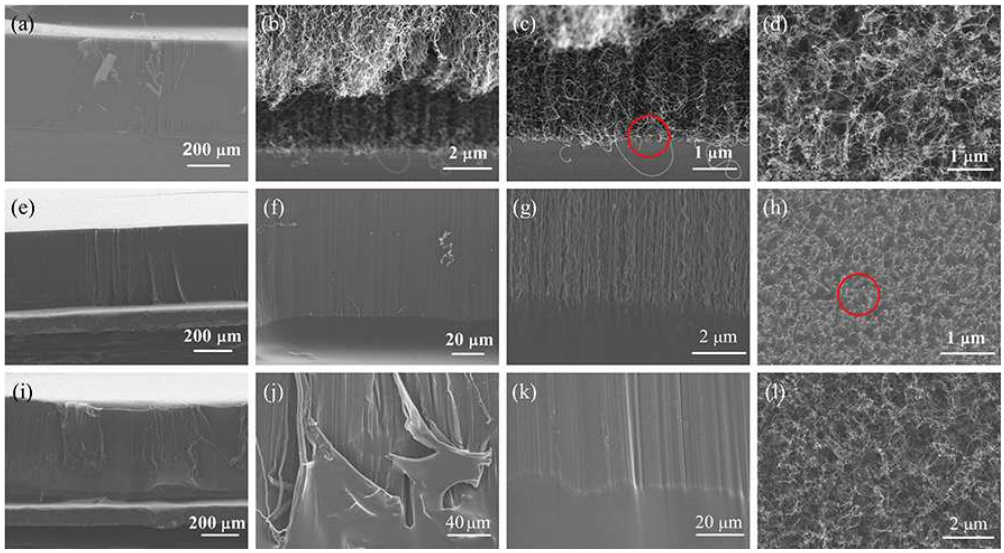


**Fig. 2** SEM images of interfacial bonding of AC (a-c), TC (e-g), and BC (i-k); SEM images of top surfaces of AC (d), TC (h), and BC (l).

SEM images of AC, TC, and BC samples showing the typical top surfaces and interfacial bonding morphology are presented in Fig. 2. Figs. 2a-2c exhibit the interfacial connection between the VACNTs and silicon substrates. It can be seen that CNTs only touch the flat surface of the silicon substrate, and the edge of the VACNT array even get detached from the substrate. Some nanoparticles (red circle in Fig. 2c) can be found near the bottom of the VACNT array, which support that the base-growth mechanism of VACNT arrays is available.[33] CNTs on the top surface (Fig. 2d) are randomly distributed; they are curly and entangled, and form clusters with small clumps. Figs. 2e-2g show the interfacial bonding of TC with the polymer substrate, where the original top surface of the VACNT array was immersed in the polymer solution. SEM images illustrate that the transferred VACNT array maintained its vertically aligned structure and a large number of CNTs embedded the polymer layer (Fig. 2g). Fig. 2h shows the top morphology, which is the original bottom

surface. Compared with Fig. 2d, CNTs of the new top surface (i.e., the original bottom surface) were more uniformly distributed without obvious curly, entangled morphologies. Although CNTs no longer clustered into clumps, they can maintain their vertically aligned structure and they formed separated bundles (red circle in Fig. 2h). Figs. 2i-2k show the interfacial bonding morphologies of BC with the polymer substrate. The detached freestanding VACNT array was directly embedded into the polymer layer, keeping the vertically aligned body structure and the original top surface unchanged. Moreover, the polymer infiltrated the bottom side of CNTs and formed a good interfacial bonding, as deduced from Figs. 2j and 2k. Fig. 2l shows the top surface, which is similar to that shown in Fig. 2d, because the bottom transfer method can keep the top surface of the VACNT array unchanged.

Raman characterization was carried out to evaluate the quality of VACNT arrays. For CNTs, D band (at ~1350 $cm^{-1}$) represents disordered or amorphous carbon and G band (at ~1580 $cm^{-1}$) indicates ordered graphite.[37] As shown in Fig. 3, the G/D peak intensity ratio of both BC and AC are near 0.85, indicating that oxidation will not change the quality of VACNT arrays. However, the G/D peak intensity ratio of TC is higher (1.32) than that of the other two surfaces. It implies that the bottom side of AC shows better properties such as good graphitization and alignment. These results are consistent with those obtained by SEM analysis. Through the proposed transfer method, transferred VACNT arrays with different top morphology can be obtained, thus providing a further option for using VACNT arrays for different applications.

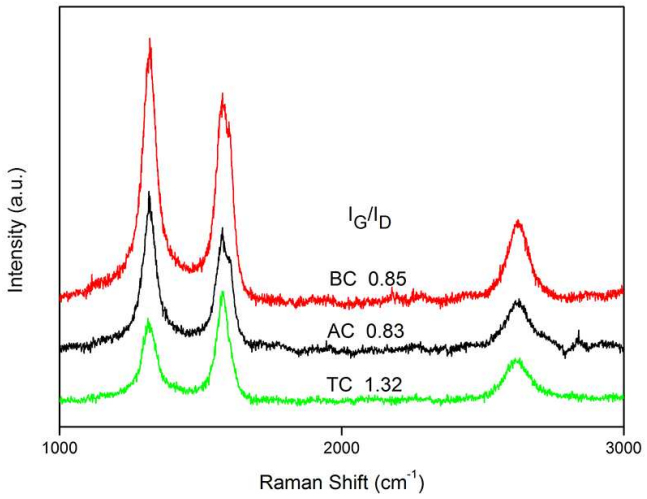


**Fig. 3** Micro-Raman spectra of AC, TC, and BC samples.

### 3.2 Interfacial adhesive strength test of transferred VACNT array

AC, TC, and BC samples (5 mm x 5 mm, length ~400 μm; red circle in Fig. 4a) were finger-pressed onto the glass surface as shown in Fig. 4a. Fig. 4b shows the hanging strength calculated based on the hanging weights of AC, TC, and BC (10 samples per group) and Fig. 4c1 schematically illustrate the test system. The results show that AC can support nearly 50 g weights only and the hanging strength is around 2 N/cm$^2$. When the weight were further increased, the VACNT array suddenly detached from the silicon substrate, leaving the main VACNT array still adhering on to the glass surface (schematically illustrated in Fig. 4c2. This is because the interface bonding between the VACNT array and the silicon substrate of AC is so weak that only a small amount of weights can be suspended. As soon as the hanging weights became greater than the interfacial bonding strength (around 2 N/cm$^2$), the VACNT array was detached from the silicon substrate. However, the contact between the CNTs and the glass surface was still intact (after the detachment) and the silicon

substrate was still adhered to the PET sheet.

For the adhesion test of TC samples, the maximum hanging weights was increased to around 550g (20 N/cm$^2$). On further increasing the weights, the TC sample got detached from the glass substrate, leaving some CNT residues attached to the glass surface. In this step, the detachment occurred between the VACNTs and the glass surface (schematically illustrated in Fig. 4c3). Compared with AC, the interfacial bonding strength between VACNTs and the PET sheet was enhanced dramatically (>20 N/cm$^2$). During the test, the shear adhesive strength of TC with glass surface was near 20 N/cm$^2$, which was lower than the interfacial bonding strength of TC and the adhesive strength of the 3M scotch tape.

For testing the BC samples, the sustained weights of 850 g (32 N/cm$^2$) can be achieved, which is higher than that for TC (20 N/cm$^2$). To our surprise, on increasing the weights, the detachment occurred between the 3M scotch tape and the plastic sheet. The BC sample was still firmly adhered to the glass surface (schematically illustrated in Fig. 4c4). This interesting result implies that both the adhesive strength between VACNTs and the glass surface and the interfacial bonding strength of BC were stronger than the hanging strength (32 N/cm$^2$), thus breaking the interface between the 3M adhesive and the plastic sheet. At the same time, BC samples exhibited a stronger adhesion than TC samples and an obviously increased interfacial bonding strength compared with that of AC.

The SEM images in Fig. 2 show that CNTs on the top surface of the BC samples (Fig. 2l) are arranged more disorderly than on TC samples (Fig. 2h). The curly,

entangled, and randomly distributed CNTs can help increase the contact area of the BC samples during finger-pressed preloading, while the uniformly distributed CNTs made more point-by-point contact with the glass surface, thus decreasing the contact area of the TC samples. It is known that the contact area of fibers with a substrate is related to the adhesive strength;[38-39] therefore, the higher contact area of the BC samples, the higher the adhesive strength. In addition, due to increase in interfacial bonding after the transfer process, the structural stability and adhesive strength of the BC and TC samples also increased, and thus, they show the potential to be used as gecko-inspired dry adhesive materials.

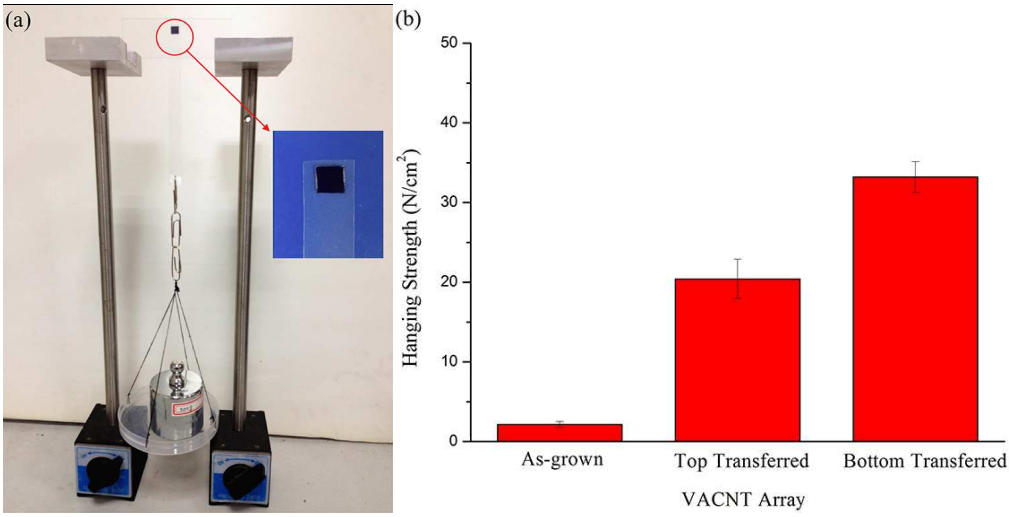

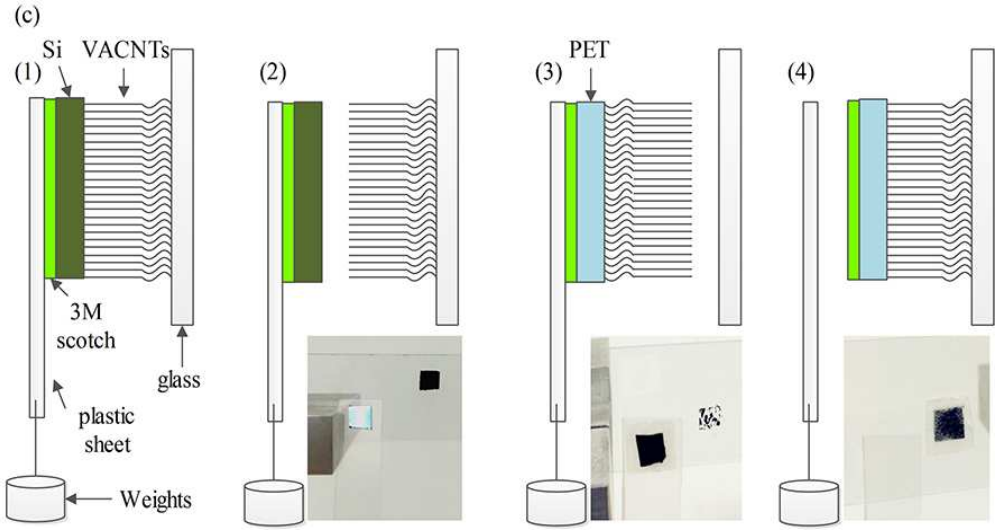


**Fig. 4** Adhesion tests of VACNT array with the hanging weights system. (a) Photograph of the hanging weights system; (b) Shear adhesive strength of AC, TC, and BC samples and 10 samples were tested for AC, TC, and BC, respectively. The preload strength was nearly 40 N/cm$^2$ by finger-press; (c) Schematics of different test states of AC, TC, and BC: (1) Adhesion state of AC (hanging 50 g weights). (2) Detachment of AC (hanging over 50 g weights and separation between silicon substrate and CNTs). (3) Detachment of TC (hanging over 550 g and separation between CNTs and glass slide). (4) Detachment of BC (hanging over 850 g and separation between plastic sheet and 3M adhesive).

### 3.3 Shear adhesive behavior of transferred VACNT array

The TC and BC samples (length ~400 μm ) were designed to 5 mm × 5 mm size and mounted on the sample stage of the multifunctional material adhesion and friction test platform (Fig. 5a) to precisely investigate the shear adhesive behavior. The whole test process is schematically illustrated in Fig. 5b as described in experimental part.

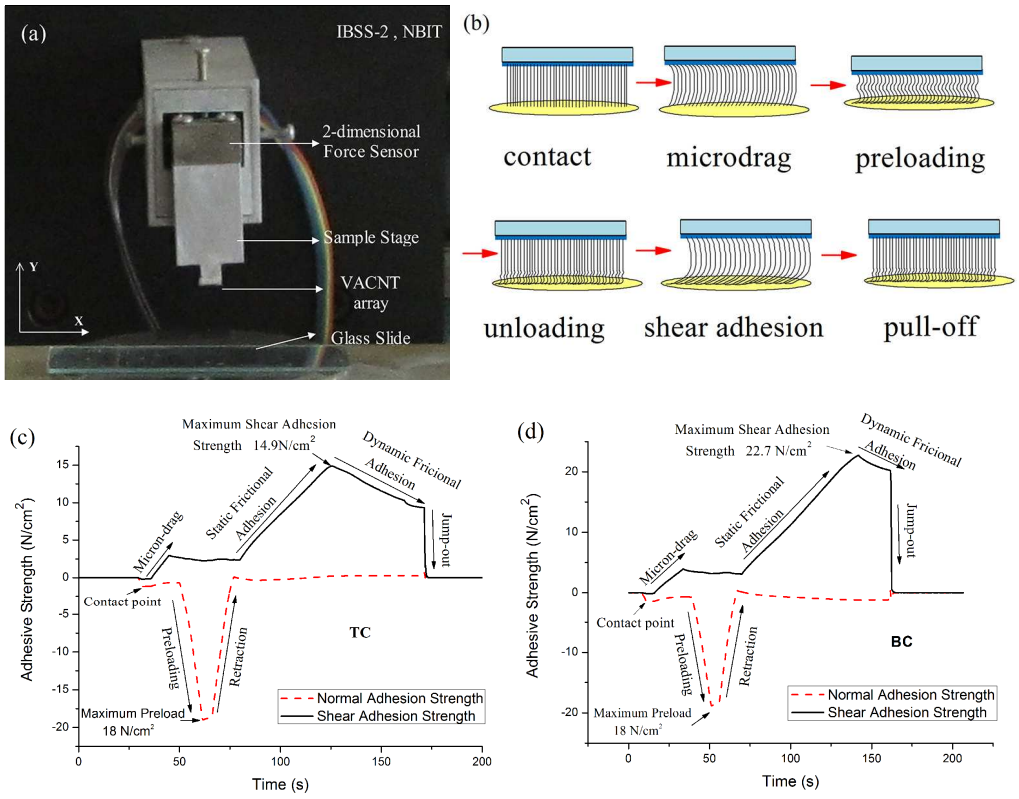


**Fig. 5** (a) Adhesion test of VACNT array with the multifunctional material adhesion and friction test platform (IBSS-2, NBIT, Nanjing, CHINA); (b) Schematics of preloading, retraction, and shear frictional test; Variations of adhesive strength as a function of movement time of TC sample (c) and BC sample (d).

The relationships between the adhesive strength and the movement time are shown in Figs. 5c and 5d, which were obtained by measuring the shear adhesive force under preloading, retraction, and shear friction processes of TC and BC samples. Both the samples exhibited a similar adhesive behavior: a microdrag was conducted at the contact point and then the loading and unloading of the preload (18 N/cm$^2$) was completed. When the preload was completely retracted and continued to move along the interfacial direction, the shear adhesive strength increased monotonically with time, which is a static frictional adhesion process. After the maximum value of the

shear adhesive strength was reached, a plateau with a slightly decreased value was obtained for a few seconds, which is considered as the stick-slip phenomenon, during the dynamic frictional adhesion process of CNT hairs.[40] The shear adhesive strength then quickly decreased, which indicates that the dry adhesive slipped and jumped-off. The values of the maximum shear adhesive strength were approximately 14.9 and 22.7 N/cm$^2$ for the TC and BC samples, respectively. The values of the adhesion coefficient λ (the ratio of adhesive strength to preload strength) were 0.83 and 1.26 for the TC and BC samples, respectively. The shear adhesive strength of the BC sample is higher than that of the TC sample and even that of natural gecko foot (~10 N/cm$^2$,[41]). It is obviously that BC show much more potential in the gecko-inspired dry adhesive application. Thus, for the interfacial bonding test with Nanoscratching method and self-cleaning ability test in the following discussion, BC and AC samples were chosen to be contrasted and analyzed. Compared with the hanging strength (20 and 32 N/cm$^2$ of TC and BC samples, respectively), the shear adhesive strength obtained by test platform was somewhat less. This occurred probably because of the use of a different preloading process between the two test methods. It has been widely proved that the adhesive strength increases with increasing preload.[42,43] For finger-press preloading in a hanging weights system, the preload (40 N/cm$^2$) is far stronger than 18 N/cm$^2$ provided by the sample stage (which is limited by the maximum measure range of force sensor, which is 5 N), thus enhancing the adhesive strength results of hanging weights system. The effect of preload on adhesive strength of BC and TC samples was also investigated with the test platform, as shown in Fig. S4 in the supporting

information, and the adhesive strengths increased with applied preload strength. It is well known that Van der Waals forces are mainly responsible for the adhesive property of CNTs[10] and increasing the contact area between CNTs and surface will help enhancing the adhesive strength.[38,39] Thus, increasing the preload strength will bring more contact area between CNTs and glass surface and further enhancing the adhesive strength of VACNT array. Meanwhile, compared with the rigid and flat surface of the sample stage, the finger surface is soft and adaptable, which could further promote the real contact area between CNTs and the test surface and thereby increase the adhesive strength. The adhesive behavior under a certain preload is quite important for precisely controlling the adhesion of CNT array-based dry adhesive materials used for fabricating gecko-mimetic climbing robots.

### 3.4 Nanoscratching tests for interfacial bonding

The nanoscratch method was used to quantitatively characterize the interfacial bonding strength between VACNT arrays with different substrates. As shown in Fig. 6a, 150-μN preload was applied during the nanoscratch between 20 and 120 μm scratch distances. For the AC and BC samples, the nanoscratch process was started from the bare substrate, resulting into scratched VACNT arrays. Fig. 6c shows the lateral force on tip versus scratch distance for AC and bare silicon substrate. When the indenter tip faced CNTs on the silicon substrate, the lateral force suddenly increased to ~120 μN and then maintained a constant response during the entire scratch process. On the bare silicon substrate, the lateral force on tip was kept around 50 μN. The

SEM image of the scratched AC is depicted in Fig. 6e, which shows that CNTs were completely uprooted and removed from the silicon substrate and formed a triangular space with CNTs rolled upward. Fig. 6d (for BC and bare PET substrate) shows that when moving through the bare PET substrate, the lateral force increased to 400 μN compared with the scratch on the bare Si substrate (50 μN) because of the presence of a TPU layer spin coated on the top surface of the PET substrate. The surface of TPU layer is rougher than the silicon substrate with $Al_2O_3$/Fe layers; as a result, it increased the friction of the indenter tip. For the BC sample, the lateral force increased linearly with the scratch distance on facing the VACNT array, and the maximum lateral force was nearly 2250 μN. From the SEM image shown in Fig. 6f, it is clear that VACNTs transferred by the TPU layer on the PET substrate detached incompletely and accumulated at the front edge of the indenter tip, leading to a linear increase in the lateral force. From the lateral force plots and SEM images, it is obvious that CNTs transferred onto the PET substrate exhibited a stronger interfacial bonding; as a result, CNTs cannot be easily detached from the substrate by the indenter tip. This result is further illustrated in Fig. 6b, which shows increments in the lateral force for the AC and BC samples plotted for 10 scratches per sample; the schematic of the nanoscratch process is shown in the inset. The increased lateral force can represent the interfacial bonding between VACNTs with different substrates.[25] The increment of BC is much higher (15 times) than that of AC, which implies that the transfer method proposed here indeed enhanced the bonding strength and structural stability of the VACNT array applied as a gecko-inspired dry adhesive material.

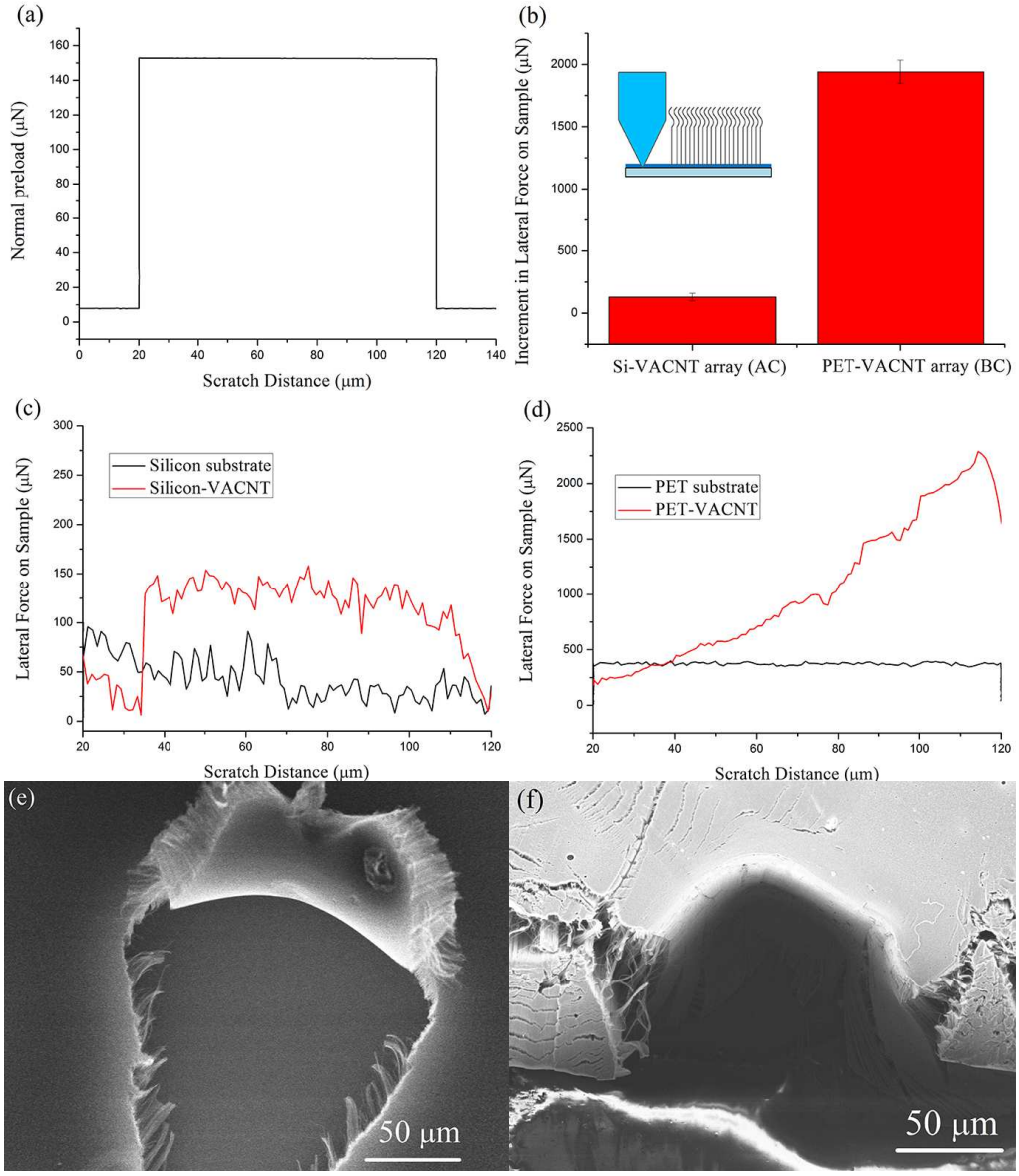


**Fig. 6** Nanoscratch of VACNT array for interfacial bonding test. (a) Normal preload (150 μN) of the Nano Indenter during scratching; (b) Increment in lateral force for AC and BC; the inset schematically illustrates nanoscratch process; (c) Lateral force on AC and bare Si substrate versus scratch distance; (d) Lateral force on BC and bare PET substrate versus scratch distance; SEM images of AC (e) and BC (f) after nanoscratch tests.

### 3.5 Self-cleaning property of transferred VACNT array based dry adhesive materials

Figs. 1b and 1d show that AC samples cannot be folded or curled whereas BC samples could be, in a manner similar to the movement of the gecko foot pad shown by Hu et al.[32] Thus, it can be assumed that the transfer method presented in our study could be beneficial for fabricating VACNT arrays that could through mimicking the DH motion of geckos to promote their dynamic self-cleaning performance as an outstanding CNT array-based dry adhesive materials. Figs. 7a and 7b show that the mimetic DH and LM motion with tweezers as described in experimental section. SEM images of the contaminated top surfaces of the AC and BC samples are shown in Figs. 7c and 7e, respectively, where silicon particles are densely adhered to their top surfaces. Figs. 7d and 7f show the SEM images of the top surfaces of the AC and BC samples after repeating the mimetic DH and LM motion. The BC sample shows a cleaner and clearer surface with only a few small silicon particle residues compared with those in the AC sample. Although the self-cleaning ability cannot be quantitatively evaluated by only contrasting the SEM images, it is still obvious evident that the top surface of the BC sample exhibited a greater nonfouling state with only fewer and smaller silicon particles left on top. This result proves that the VACNT array transferred onto the flexible substrate can mimic the DH motion of geckos to exhibit a better nonfouling state, which shows that the VACNT array owns better potential for developing a self-cleaning ability similar to that possessed by geckos.

It has been proved that with DH motion, dynamic self-cleaning mechanism could help gecko surmount substantially higher adhesion force between the setae and particles than that without DH motion.[32] During the hyperextended motion, setae

arrays with spatula on top were roll up and spread out progressively from the substrate. This scrolling motion accumulate elastic energy in each contacting setae within the peeling zone and finally lead to a dynamically jump-off and then generate inertial force high enough to dislodge dirt particles. The dynamic effect could also be used to interpret the scrolled and peeled transferred VACNT array samples with better non-fouling state. The AC sample could not be scrolled and was directly detached from the glass substrate, thus no elastic energy accumulation and jump-off process happened.

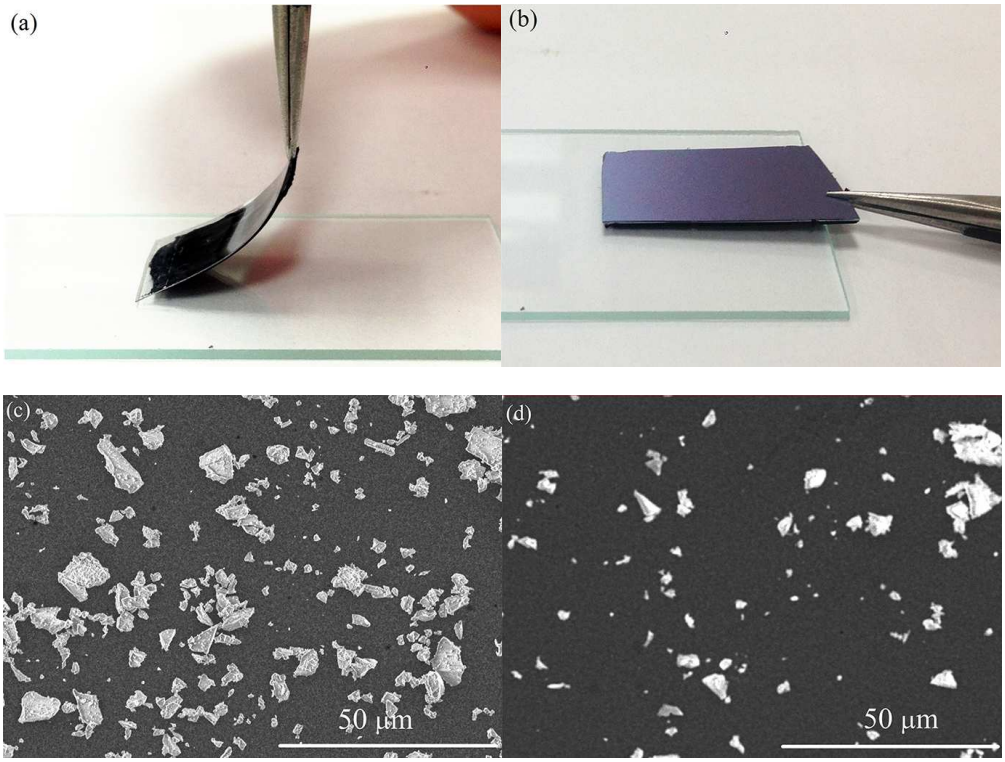

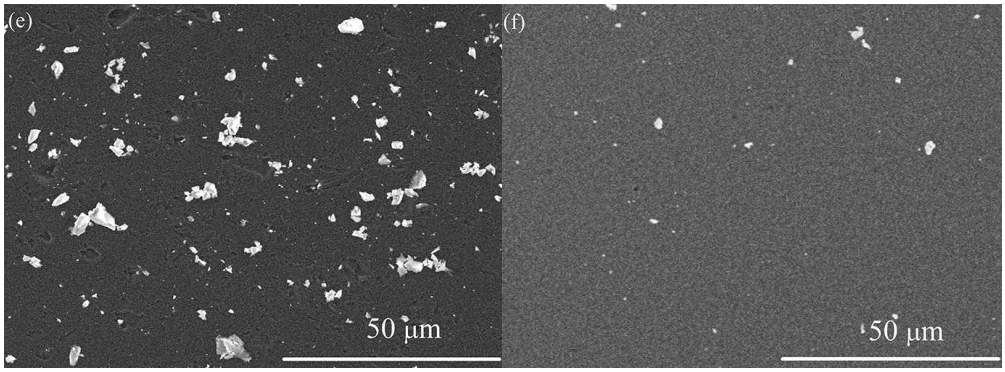


**Fig. 7** Mimicking the DH motion of gecko foot by shaking AC (a) and scrolling BC (b); SEM images of AC (c) and BC (d) contaminated by silicon particles; SEM images of the self-cleaned state of AC (e) and BC (f) through mimicking the digital hyperextension of live gecko.

However, the mechanism of the self-cleaning ability owned by geckos is still not completely understood. Increasing attention has been paid to investigate this mechanism deeply, and some other self-cleaning mechanisms have also been investigated, such as the lotus effect,[44,45] contact self-cleaning with energy disequilibrium,[46-48] and even the chemical secretion of gecko's footprints has been considered.[49] Therefore, the DH motion could not be the only reason responsible for the self-cleaning ability and the other factors that could affect the self-cleaning ability of VACNT array need to be considered in the future work.

## 4. Conclusion

In summary, we have presented a transfer method to fabricate VACNT array-based dry adhesive materials onto a flexible PET substrate with TPU as the intermedium. A thermal oxidation process was introduced to obtain freestanding VACNT arrays, resulting in the production of top-transferred and bottom-transferred

structural VACNT array-based dry adhesive materials. Interfacial bonding strength of the transferred VACNT array was enhanced dramatically, and an improved adhesive behavior were exhibited. The flexible structure of the transferred VACNT array showed a better nonfouling state by mimicking the DH motion of the gecko foot. We obtained a stable structure of VACNT array-based dry adhesive materials with strong interfacial bonding, high adhesive strength, and ability to keep nonfouling state, conditions that are favorable for using VACNT arrays as gecko-inspired dry adhesives. This work reveals a new direction for the biomimetic design of VACNT array-based gecko-inspired dry adhesive materials with high reusability and reliable properties. Although more efforts are required for achieving a better understanding of this issue, we still believe that transferring the VACNT array onto flexible substrates is the first step for the application of CNT array-based dry adhesive materials.

## Acknowledgment

This work was supported by National Natural Science Foundation of China (No.51275237, No. 51372265, and No.51435008 (key project)), the Natural Science Foundation of Jiangsu Province, China (No. BK20140392), and the Project Funded by the Priority Academic Program Development of Jiangsu Higher Education Institutions.

## References


1 A. P. Russell, *Integr. Comp. Biol.*, 2002, **42**, 1154–1163.

2 K. Autumn, N. Gravish, *Philos. T. R. Soc. A*, 2008, **366**, 1575–1590.

3 K. Autumn, M. Sitti, Y. A. Liang, A. M. Peattie, W. R. Hansen, S. Sponberg, T. W. Kenny, R. Fearing, J. N. Israelachvili and J. R. Full, *Proc. Natl. Acad. Sci.*, 2002, **99**, 12252–12256.

4 Z. d. Dai, J. R. Sun, *J. Bionic. Eng.*, 2007, **4**, 91–95.

5 L. Q. Dai, H. Zhang and Z. D. Dai, *Robot*, 2008, **30**, 182-186.

6 M. Carlo, S. Metin, *J. Bionic. Eng.*, 2006, **3**, 115–125.

7 M. Sitti, R. S. Fearing, *J. Adhes. Sci. Technol.*, 2003, **17**, 1055–1073.

8 Y. Mengüç, S. Y. Yang, S. Kim, J. A. Rogers and M. Sitti, *Adv. Funct. Mater.*, 2012, **22**, 1246–1254.

9 H. Lee, B. Bhushan, *J. Colloid. Interf. Sci.*, 2012, **372**, 231–238.

10 L. T. Qu, L. M. Dai, M. Stone, Z. H. Xia and Z. L. Wang, *Science*, 2008, **322**, 238–242.

11 L. H. Ge, S. Sethi, L. J. Ci, P. M. Ajayan, A. Dhinojwala, *Proc. Natl. Acad. Sci.*, 2007, **104**, 10792–10795.

12 Y. Li, H. Zhang, G. Xu, L. Gong, Z. Z. Yong, Q. W. Li and Z. D. Dai, *SPIE Smart Structures and Materials+ Nondestructive Evaluation and Health Monitoring*, San Diego, 2013.

13 M. P. Murphy, B. Aksak and M. Sitti, *Small*, 2009, **5**, 170–175.

14 H. E. Jeong, J. K. Lee, H. N. Kim, S. H. Moon and K. Y. Suh, *Proc. Natl. Acad.*

*Sci.*, 2009, **106**, 5639–5644.

15 M. Sitti, R. S. Fearing, *J. Adhes. Sci. Technol.*, 2003, **17**, 1055–1073.

16 B. Aksak, M. P. Murphy and M. Sitti, *Langmuir*, 2007, **23**, 3322–3332.

17 M. S. Dresselhaus, G. Dresselhaus and P. C. Eklund, Elsevier, San Diego CA, 1996, pp. 765–802.

18 J. M. Bonard, J. P. Salvetat, W. A. Stockli T, de Heer, L. Forró and A. Châtelain, *Appl. Phys. Lett.*, 1998, **73**, 918–920.

19 T. Dürkop, S. A. Getty, E. Cobas and M. S. Fuhrer, *Nano Lett.*, 2004, **4**, 35–39.

20 Z. Yao, C. L. Kane and C. Dekker, *Phys. Rev. Lett.*, 2000, **84**, 2941–2944.

21 J. Hone, M. Whitney and A. Zettl, *Phys. Rev. B*, 1999, **59**, 2514–2516.

22 Y. Zhao, T. Tong, L. Delzeit, A. Kashani, M. Meyyappan and A. Majumdar, *J. Vac. Sci. Technol. B*, 2006, **24**, 331–335.

23 M. F. Yu, T. Kowalewski and R. S. Ruoff, *Phys. Rev. Lett.*, 2001, **86**, 87–90.

24 Y. Zhu, X. D. Lim, M. C. Sim, C. T. Lim and C. H. Sow, *Nanotechnology*, 2008, **19**, 325304.

25 I. Lahiri, D. Lahiri, S. Jin, A. Agarwal and W. Choi, *ACS Nano*, 2011, **5**, 780–787.

26 K. Autumn, C. Majidi, R. E. Groff, A. Dittmore and R. Fearing, *J. Exp. Biol.*, 2006, **209**, 3558–3568.

27 A. Abdelhalim, A. Abdellah, G. Scarpa and P. Lugli, *Carbon*, 2013, **61**, 72–79.

28 J. Mäklin, N. Halonen, O. Pitkänen, G. Tóth and K. Kordás, *Appl. Therm. Eng.*, 2014, **65**, 539–543.

29 S. J. Kang, C. Kocabas, H. S. Kim, Q. Cao, M. A. Meitl, D. Y. Khang and J. A. Rogers, *Nano lett.*, 2007, **7**, 3343–3348.

30 P. Mishra, N. H. Tai and S. S. Harsh, Islam, *Mater. Res. Bull.*, 2013, **48**, 2804–2808.

31 B. Aksak, M. P. Murphy and M. Sitti, *IEEE International Conference on. IEEE* 2008, 3058-3063.

32 S. Hu, S. Lopez, P. H. Niewiarowski and Z. Xia, *J. R. Soc. Interface*, 2012, **9**, 2781–2790.

33 R. T. K. Baker, *Carbon*,1989, **27**, 315–323.

34 P.X. Hou, C. Liu and H. M. Cheng, *Carbon*, 2008, **6**, 2003–2025.

35 M. Wang, T. T. Li, Y. G. Yao, H. F. Lu, Q. Li, M. H. Chen and Q. W. Li, *J. Am. Chem. Soc.*, 2014, **136**, 18156–18162.

36 M. Wang, H. Y. Chen, Y. J. Xing, H. X. Wei, M. H. Chen, Q. W. Li and Xuan Y. M. *J. Nanosci. Nanotechno.*, 2015, **15**, 3212–3217.

37 L. Nilsson, O. Groening, C. Emmenegger, O. Kuettel, E. Schaller, L. Schlapbach, H. Kind, J-M. Bonad and K. Kern, *Appl. Phys. Lett*., 2000, **76**, 2071–2073.

38 J. Lee, C. Majidi, B. Schubert and R. S. Fearing, *J. Roy. Soc. Interface*, 2008, **5**, 835–844.

39 C. S. Majidi, R. E. Groff and R. S. Fearing, *J. Appl. Phys.*, 2005, **98**, 103521.

40 L. H. Ge, L. J. Ci, A. Goyal, R. Shi, L. Mahadevan, P. M. Ajayan and A. Dhinojwala, *Nano Lett.*, 2010, **10**, 4509–4513.

41 K. Autumn, Y. A. Liang, S. T. Hsieh, W. Zesch, W. P. Chan, T. W. Kenny, R.

Fearing and R. J. Full, *Nature*, 2000, **405**, 681–685.

42 Y. Cui, Y. Ju, B. Xu, P. Wang, N. Kojima, K. Ichioka and A. Hosoi, *RSC Adv.*, 2014, **4**, 9056–9060.

43 Y. Maeno, Y. Nakayama, *J. Adhesion*, 2012, **88**, 243–252.

44 W. Barthlott, C. Neinhuis, *Planta*, 1997, **202**, 1–8.

45 C. Neinhuis, W. Barthlott and *Ann. Bot.*, 1997, **79**, 667–677.

46 U. A. Abusomwan, M. Sitti, *Langmuir*, 2014, **30**, 11913–11918.

47 Y. Mengüç, M. Röhrig, U. Abusomwan, H. Hölscher and M. Sitti, *J. R. Soc. Interface*, 2014, **11**, 20131205.

48 W. R. Hansen, K. Autumn, *Proc Natl Acad Sci U.S.A.*, 2005, **102**, 385–389.

49 P. Y. Hsu, L. H. Ge, X. P. Li, A. Y. Stark, C. Wesdemiotis, P. H. Niewiarowski and A. Dhinojwala, *J. R. Soc. Interface*, 2012, **9**, 657–664.